Electronic Supplementary Information (ESI).

C@MoO_2 hollow yolk-shell structure with excellent Electrochemical Properties as Faradaic Electrode

Arka Saha,[a] Aniruddha Mondal,[a] Sandipan Maiti,[b] Subhash C. Ghosh,[a] Sourindra Mahanty,[b]* and Asit Baran Panda [a]*

[a] *Central Salt and Marine Chemicals Research Institute (CSIR-CSMCRI) and CSMCRI- Academy of Scientific and Innovative Research, G. B. Marg, Bhavnagar-364002, Gujarat, India. E-mail: abpanda@csmcri.org.*

[b] *CSIR-Central Glass & Ceramic Research Institute, Raja S C Mullick Road, Kolkata-700032, India.E-mail: mahanty@cgcri.res.in*

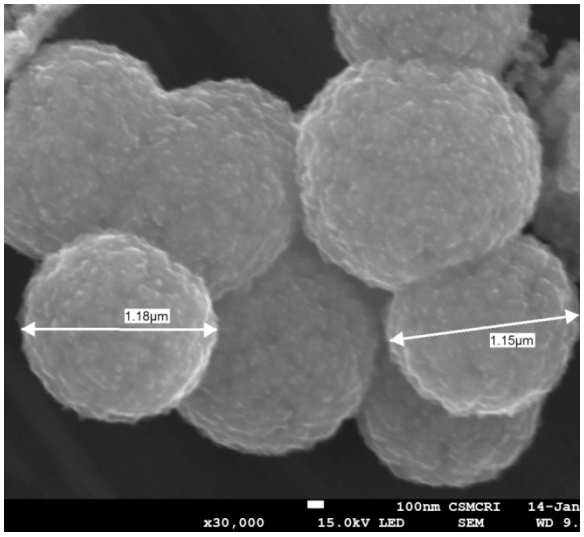

Fig. S1 FE-SEM image of the as-synthesized C@MoO_2.

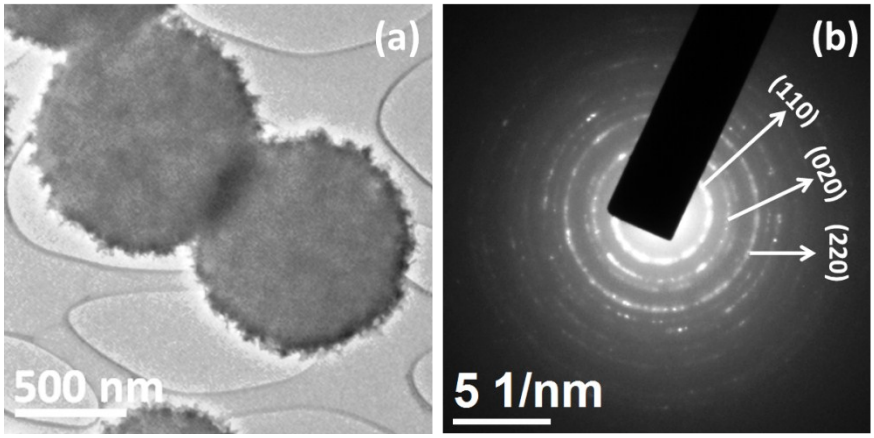

Fig. S2 (a) TEM image of as-synthesized C@MoO_2 and (b) SAED pattern of calcined C@MoO_2.

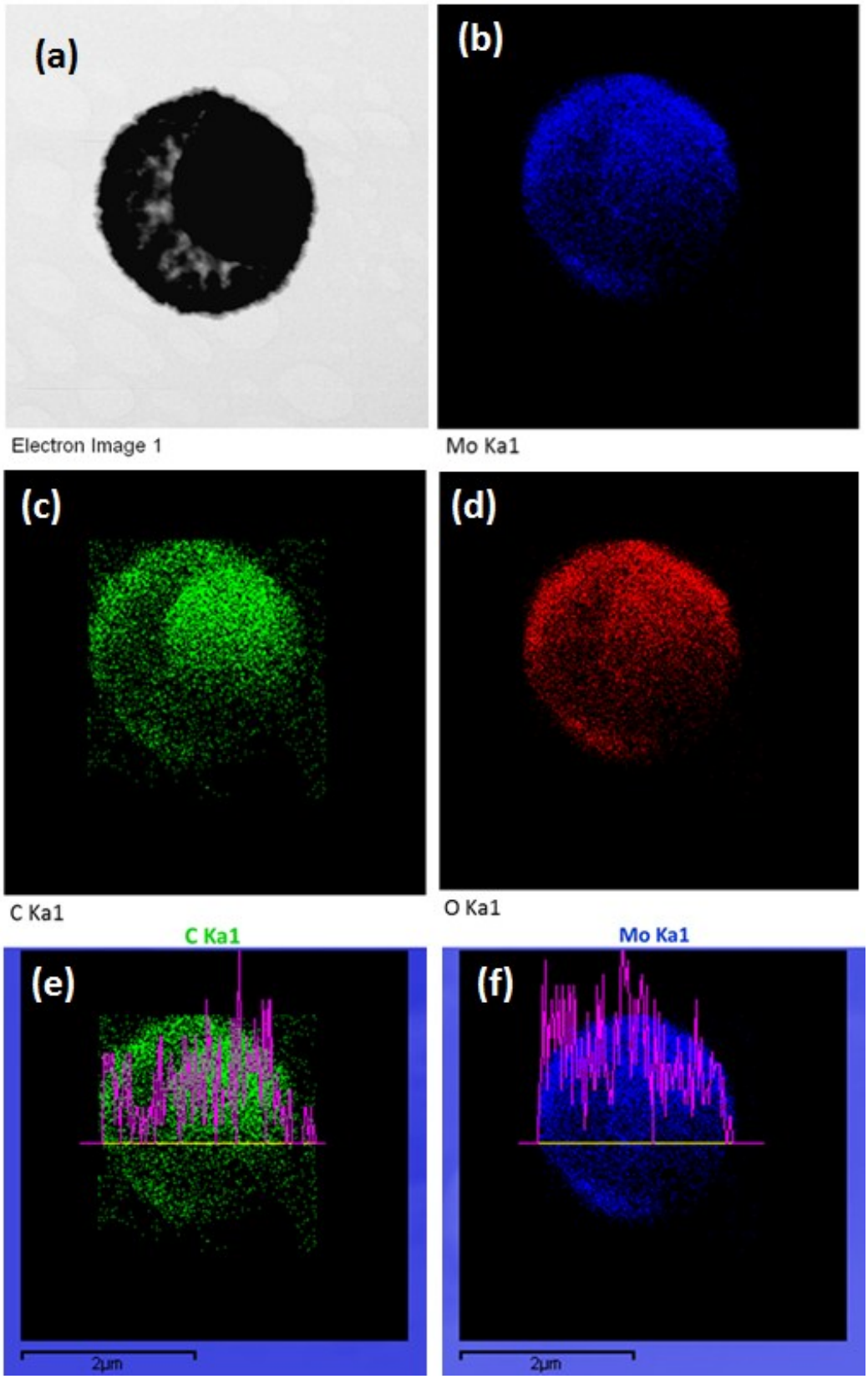

Fig. S3 (a)TEM image (b-d) elemental mapping image and (e-f) corresponding EDX line scan image of calcined C@MoO_2 hollow spheres.

The TEM image Fig.S3(a) confirmed the formation of hollow yolk-shell structure. The corresponding elemental mapping images Fig.S3(b-d) distinctly indicate that carbon is present in throughout the sphere but density of carbon in inner yolk is more. Whereas, Mo and O is homogeneously distributed in throughout the spheres. Similarly, in corresponding line scan Fig.S3(e-f) evidenced that concentration of carbon in yolk is high than that of shell and concentration of Mo in shell is more than that of core. However, it is hard to get exact information about the composition of inner yolk, as the size of the sphere is very high. Corresponding EDX elemental analysis result indicate the presence of ~8wt% of carbon in the sphere.

Although, the amount and ratio of Mo and O in the EDX elemental analysis result is in good agreement as expected, but surprisingly the amount of C is quite low (~8 wt %) than that of amount obtained from TG analysis (22%). This conformed that inner yolk contains majority of carbon, which is beyond the identification reach of EDX.

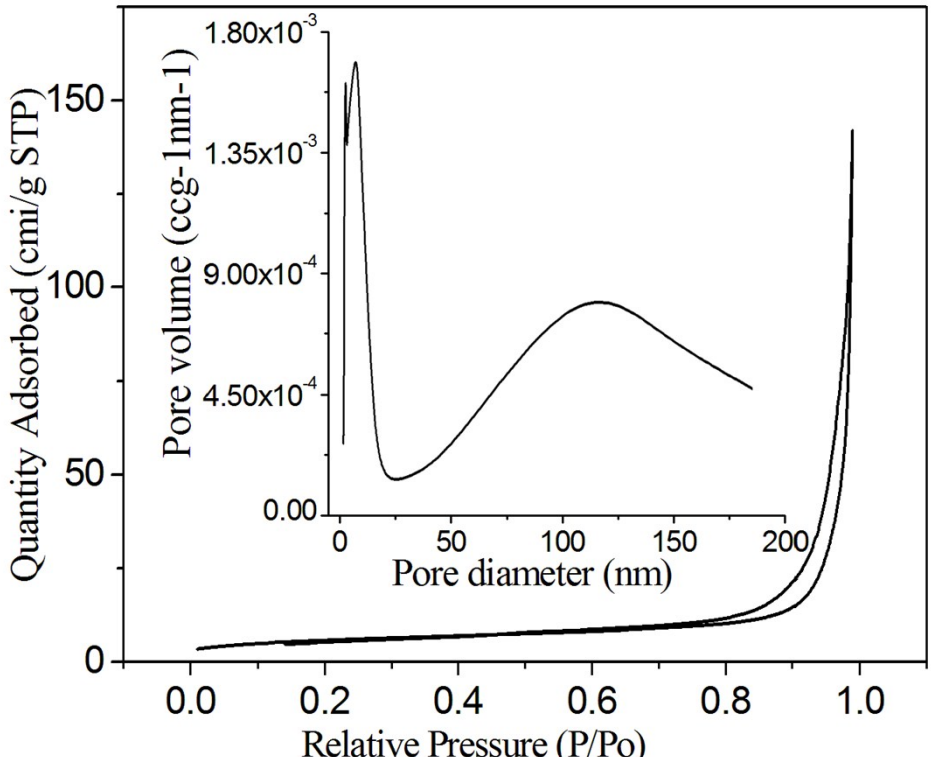

Fig. S4 The nitrogen sorption isotherm and the corresponding pore size distribution curve (inset) of calcined C@MoO_2 sample.

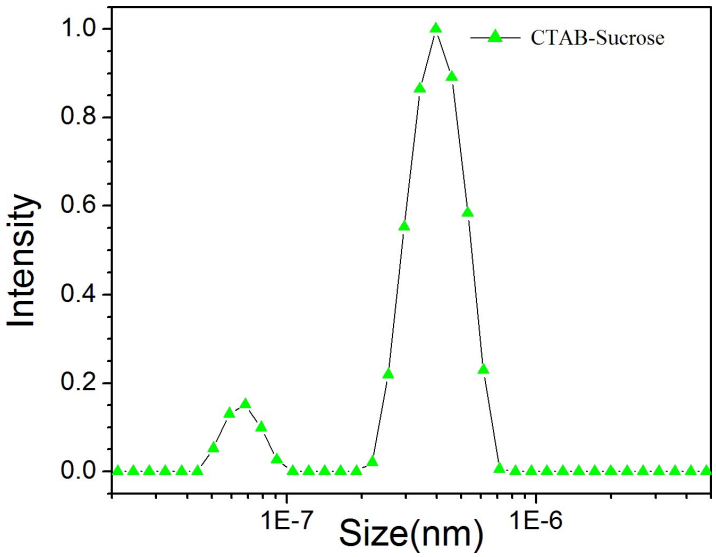

Fig. S5 The obtained average size of soft template *in-situ* formed through the CTAB-Sugar interaction obtained in the DLS measurement.

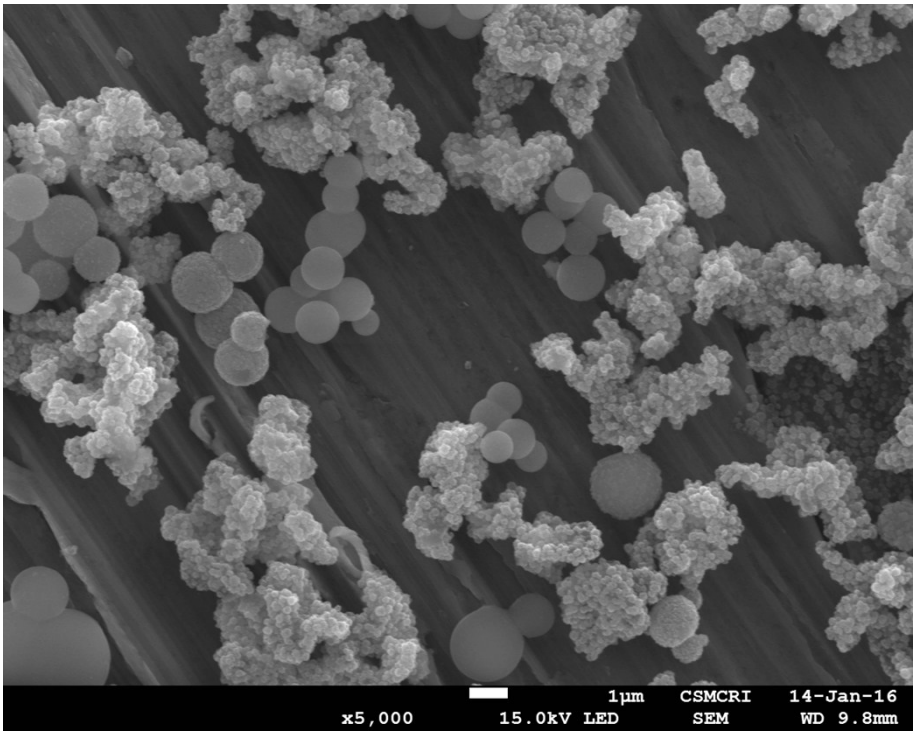

Fig. S6 Phase separated carbon sphere with randomly distributed MoO_2 nano particle formed when ammonium hydroxide was used instead of ammonium carbonate.

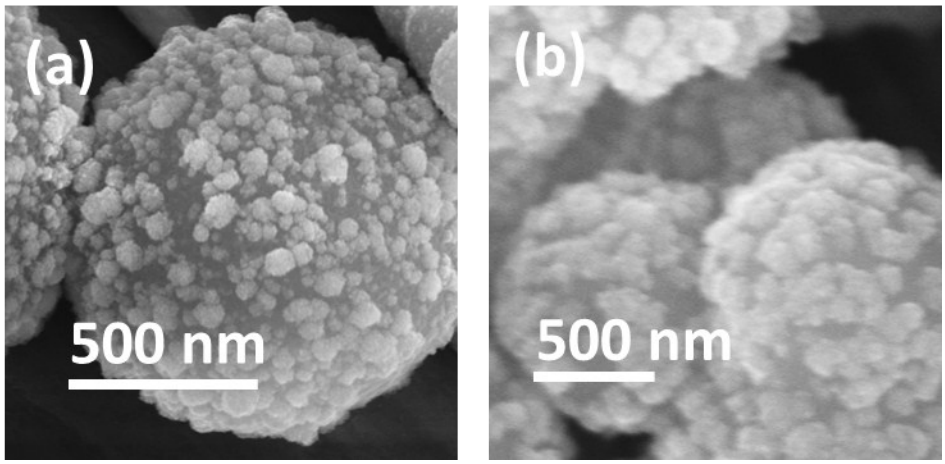

Fig. S7 SEM images of the materials formed in 4h (a) and 12h (b) with varying concentration of MoO_2 particles.

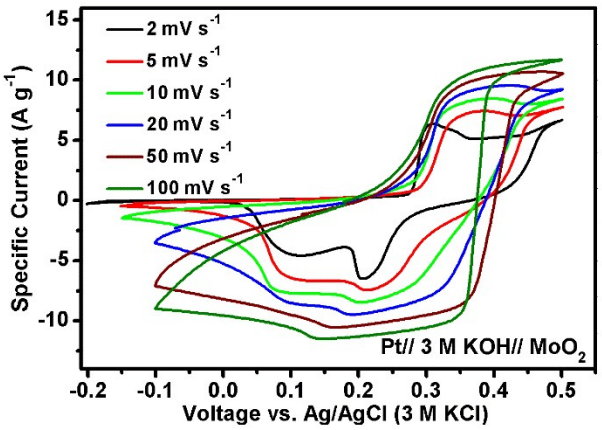

Fig. S8 The corresponding CV plots for MoO_2 at different current density.

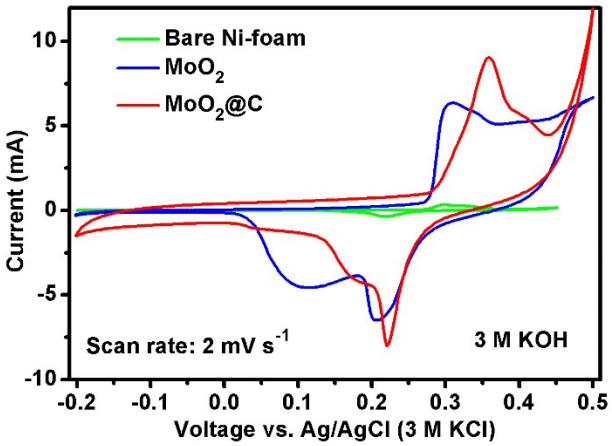

Fig. S9 Comparison of CV plots for bare Ni foam, MoO_2 and MoO_2@C at a scan rate of 2 mV s^{-1}. Calculated from the area under the curve, the overall faradic current contribution of Ni foam is ~2.5% with respect to that of MoO_2 / MoO_2@C.

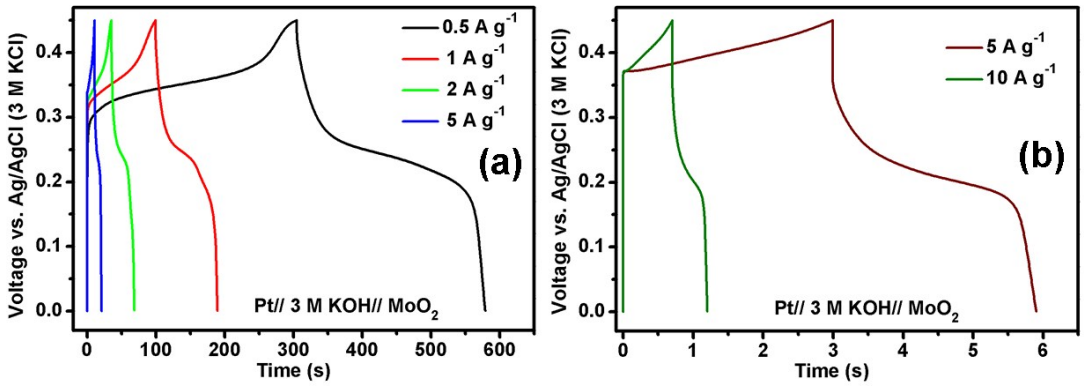

Fig. S10(a) & (b) Galvanostatic charge-discharge profiles of MoO_2 at varying current densities.

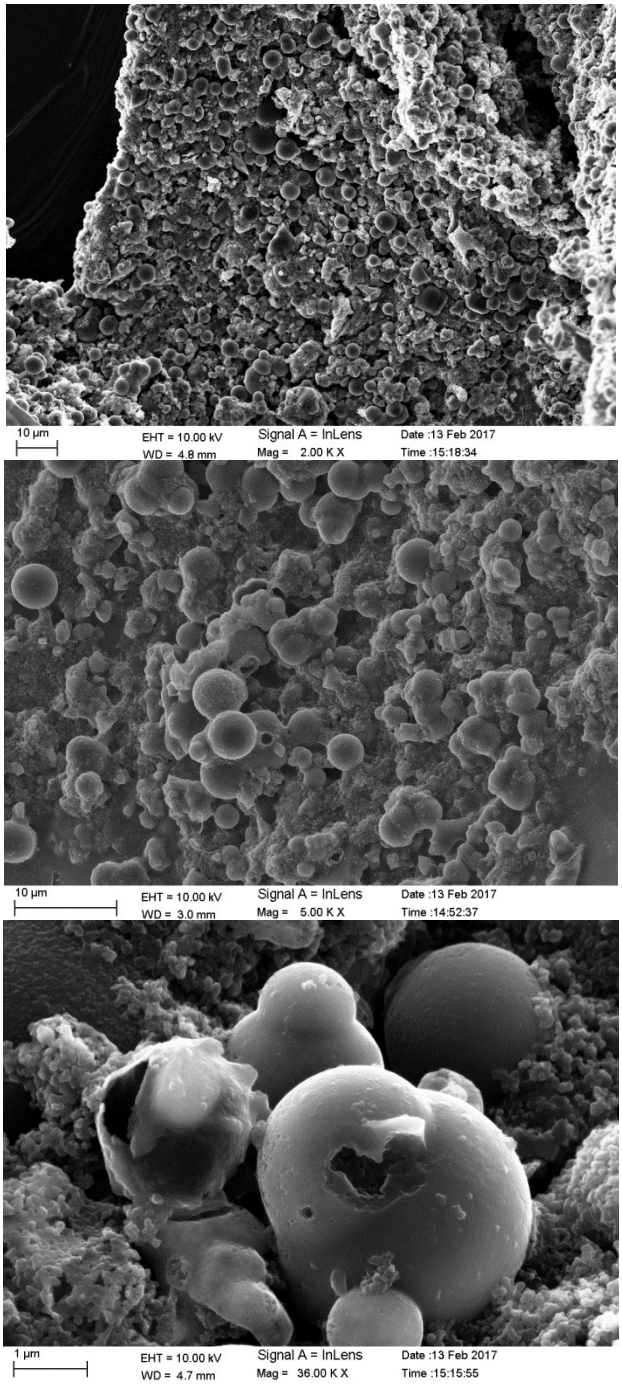

Fig. S11 FESEM micrographs of C@MoO_2 electrode film after 1000 cycles in the discharge state.

Table S1 MoO_2 based electrodes for supercapacitors.

Electrode material and loading amount	Specific Capacitance	Electrolyte used	Cycling performance	Reference
Ployanile-h-MoO_3 hollow nano rod (1mg/cm^2)	247 F/g at 1 A/g	1.0 M H_2SO_4	80% capacity retention after 5000 cycles at 50 mV/s	1
MoO_3 sheet/CNT (0.7 mg/cm^2)	540 F/g at 0.01 mV/s	1.0 M $LiCl_4$		2
h-MoO_3 0.95±0.05 mg/cm^2	230 F/g at 0.25 A/g	1.0 M H_2SO_4	74% capacity retention after 3000cycle at 50 mV/s	3
Reduced MoO_3 1.8 to 1.96 mg/cm^2	196 F/cm^3 at 0.5 A/g	5 M LiCl	89% capacity retention after 10000 cycle at 1 A/g	4
α-MoO_3 nano belt	368 F/g at 0.25 A/g	0.5 M aq. $LiSO_4$	95% capacity retention after 500 cycle at 0.25 A/g	5
α-MoO_3-graphene 10 mg/cm^2	380 F/g at 0.2 A/g	1.0 M H_2SO_4	100% capacity retention after 1000 cycle at 1 A/g	6
MoO_3/multiwall CNT 30 mg/cm^2	93 F/g at 5 mV/s	0.1 M TBAP in DMF	55% capacity retention after 800 cycle	7
Magnetron sputtered MoO_3/CNTs	70 F/g at 10 mV/s	1.0 M Na_2SO_4	82% capacity retention after 800 cycle at 100 mV/s	8
MoO_3/C hybrid 1.5 mg/cm^2	331 F/g at 1 A/g	1.0 M H_2SO_4	71 % capacity retention after 10000 cycle at 10 A/g	9
MoO_3 nano wire	288 F/g at 5 mV/s	1.0 M H_2SO_4 in ethylammonium nitrate electrolyte	96% capacity retention after 3000 cycle at 0.5 A/g	10
MoO_3 nano plate 1.5 mg in 0.4cm^2	280 F/g at 5	0.5 M $LiSO_4$	100% capacity retention after 400	11

	mV/S		cycle at 2000 mA/g	
MoO_3/Polypyrrole	129 F/g at 0.25 A/g	1.0 M Na_2SO_4	90% capacity retention after 2000 cycle at 0.67 A/g	12
RGO(MP)	553 F/g at 1mV/s	1.0 M H_2SO_4	86.6 % capacity retention after 200 cycle at 20 mV/s	13
MoO_2/SWNT	597 F/g at 10 mV/s	0.1 M Na_2SO_4	97.5 % capacity retention after 600 cycle at 10 mV/s	14
α-MoO_3 nano belts	369 F/g at 0.1 A/g	0.5 M $LiSO_4$	95% capacity retention after 500 cycle at 0.25 A/g	15
α-MoO_3 a. Microsphere b. Micro belt c. Nano rod	a. 134.9 F/g b. 91.8 F/g c. 191.2 F/g at 5 mVS^{-1}	0.1 M Na_2SO_4	Over all 70% capacity retention for all sample after 1000 cycle at 1A/g	16
C@MoO_2 yolk shell	**188 C/g (423 F/g) at 0.5 A/g**	**3M KOH**	**77% of the initial specific capacity retention after 5000 cycles at 5 Ag^{-1}**	**Present work**

Reference:

1. V. Kumar and P. S. Lee, *J. Phys. Chem.C*, 2015, **119**, 9041−9049.
2. D. Hanlon, C. Backes, T. M. Higgins, M. Hughes, A. O'Neill, P. King, N. M. Evoy, G. S. Duesberg, B. M. Sanchez, H. Pettersson, V. Nicolosi, and J. N. Coleman, *Chem. Mater.*, 2014, **26**, 1751−1763.
3. V. Kumar, X. Wang and P. S. Lee, *Nanoscale*, 2015, **7**, 11777–11786.
4. X. Xiao, C.(John) Zhang, S. Lin , L. Huang , Z. Hua, Y. Cheng , T. Li , W. Qiao , D. Long , Y. Huang , L. Mai , Y. Gogotsi , J. Zhou. Energy Storage Materials, 2015, **1**, 1–8.
5. J. Li and X. Liu., CrystEngComm, 2014, **16**, 184–190.
6. J. Zhou, J. u. Song, H. Li, X. Feng, Z. Huang, S. Chen, Y. Ma, L. Wanga and X. Yanb, *New J. Chem.*, 2015, **39**, 8780-8786.
7. L. S. Aravindaa, U. Bhatb, B. R. Bhat, *Electrochimica Acta.*, 2013, **112**, 663– 669.
8. L.S. Aravinda , K.K. Nagaraja , K. Udaya Bhat , B. R. Bhat, *Journal of Electroanalytical Chemistry*, 2013, **699**,28–32.
9. H. Ji , X. Liu , Z. Liu , B. Yan , L. Chen , Y. Xie , C. Liu , W. Hou , and G.Yang, *Adv. Funct. Mate.*, 2015, **25**, 1886–1894.

10. M. Sarfraz, M. F. A. Aboud, I. Shakir, *Journal of Alloys and Compounds*, 10.1016/j.jallcom.2015.07.274
11. W. Tang, L. Liu, S. Tian, L. Li, Y. Yue, Y. Wu and K. Zhu., *Chem. Commun.*, 2011, **47**, 10058–10060.
12. X. Zhang, X. Zeng, M. Yang, and Y. Qi, ACS Appl. Mate.Interfaces, 2014, **6**, 1125−1130.
13. X. Xia, Q. Hao, W. Lei, W. Wang, H. Wang and X. Wang, *J. Mater. Chem.*, 2012, **22**, 8314– 8320.
14. F. Gao, L. Zhang, S. Huang, *Materials Letters*, 2010, **64**, 537–540.
15. J. Jiang, J. Liu, S. Peng, D. Qian, D. Luo, Q. Wang, Z. Tiana and Y. Liu, *J. Mater.Chem. A*, 2013, **1**, 2588–2594.
16. Z. Cui, W. Yuan and C. M. Li, *J. Mater. Chem. A*, 2013, **1**, 12926–12931.